

Experimental observation of a band gap in individual Mn₁₂ molecules on Au(111)

S. Voss,^{a)} M. Fonin, and U. Rüdiger

Fachbereich Physik, Universität Konstanz, 78457 Konstanz, Germany

M. Burgert and U. Groth

Fachbereich Chemie, Universität Konstanz, 78457 Konstanz, Germany

(Received 30 January 2007; accepted 22 February 2007; published online 26 March 2007)

The authors report on the electronic properties of individual molecules of two Mn₁₂ derivatives chemically grafted on the functionalized Au(111) surface studied by means of ultrahigh vacuum scanning tunneling microscopy/spectroscopy at room temperature. Reproducible current-voltage curves were obtained from both Mn₁₂ molecules, showing a well defined wide band gap. In agreement with the tunneling spectroscopy results, the bias voltage variation upon scanning leads to apparent height changes of the Mn₁₂ clusters. The authors discuss these findings in the light of the recent band structure calculations and electronic transport measurements on single Mn₁₂ molecules. © 2007 American Institute of Physics. [DOI: 10.1063/1.2716867]

The ongoing miniaturization of electronic circuits has motivated the study of a possible use of single molecules in the design of logic or memory units of future electronic devices. Implementation of single molecules in electronic components demands an understanding of their electronic properties, which ensures the possibility to control the electronic transport through single molecule junctions. With respect to this, single molecule magnets (SMMs) such as Mn₁₂ acetate¹⁻⁴ and its derivatives combining low-temperature magnetic hysteresis and quantum effects represent a material class with a promising perspective for application in ultrahigh density data storage devices or quantum computing.⁵ During the last years, the properties of bulk SMMs have been determined to a large extent,⁶⁻⁸ whereas experiments on isolated Mn₁₂ molecules remain rare. Recent transport measurements on Mn₁₂ clusters in electromigrated break junctions revealed a SMM-like signature of the conductivity^{9,10} and a possibility for light-induced current switching in Mn₁₂ acetate.¹¹ Scanning tunneling microscopy (STM) has also been implemented to probe Mn₁₂ molecules deposited on different surfaces.^{8,12-17} However, these studies have mainly been limited to the investigation of the Mn₁₂ layer topography without addressing the electronic properties of the Mn₁₂ molecules. Moreover, the existing difficulties with the preparation of intact molecular surface layers hamper the investigation of the molecular electronic structure and transport.

Very recently, investigations of the electronic properties of Mn₁₂ derivatives bound to Au surfaces have been reported.^{18,19} The results presented in Ref. 19 showed a good agreement with recent local density approximation (LDA + *U*) calculations on the valance band structure of Mn₁₂ molecules for *U*=4 eV, confirming the presence of intact Mn₁₂ molecules on a suitably functionalized Au(111) surface. However, up to date no evidence for a band gap in a chemically intact individual Mn₁₂ cluster on a surface measured by means of scanning tunneling spectroscopy (STS) has been presented although it has been predicted theoretically^{18,20} and was observed in resonant photoemission spectroscopy

(RPES) measurements on Mn₁₂ monolayers.¹⁹

In this work, we address the electronic properties of submonolayers of Mn₁₂-thiophene-3-carboxylate [Mn₁₂O₁₂(O₂CC₄H₃S)₁₆(H₂O)₄] (Mn₁₂-th) and Mn₁₂-parafluorobenzoate [Mn₁₂O₁₂(O₂CC₆H₄F)₁₆(H₂O)₄] (Mn₁₂-pfb) chemically grafted on a Au(111) surface functionalized with 4-mercapto-2,3,5,6-tetrafluorobenzoic acid (4-MTBA) studied by STM/STS at room temperature (RT). Current voltage (*I-U*) spectra of the individual Mn₁₂ molecules exhibit a broad gap region of low conductance between two regions of increasing conductivity. Upon bias-dependent imaging qualitatively different STM images are obtained, showing a direct correlation with the spectroscopic features. These findings are discussed in the light of recent band structure calculations on Mn₁₂ acetate as well as of recent experiments on single molecules and molecular arrays.

Mn₁₂-th and Mn₁₂-pfb single crystals were prepared according to the procedure reported by Lim *et al.*²¹ and Burgert *et al.*,²² respectively. The 4-MTBA functionalization layer as well as the Mn₁₂ layers were prepared according to the procedure reported elsewhere.¹⁹ STM and STS measurements were performed in ultrahigh vacuum (UHV) with an Omicron VT AFM/STM at RT using electrochemically etched tungsten tips that were flash annealed by electron bombardment. The ± sign of the bias voltage denotes the voltage applied to the sample.

Figure 1(a) shows a STM image of Mn₁₂-th clusters on the 4-MTBA functionalized Au(111) surface. The apparent diameter of the molecules is significantly larger than the expected diameter of ~2 nm. This can be explained by the apex geometry of the blunt STM tip used in this experiment. In earlier experiments¹⁹ freshly prepared atomically sharp STM tips were also implemented, which resulted in a reduced apparent diameter of the molecules showing a good agreement with the expected value of ~2 nm, ensuring that single molecules were investigated instead of agglomerated clusters of molecules. However, we found that only blunt STM tips delivered reproducible *I-U* curves on Mn₁₂-th layers.

^{a)}Electronic mail: soenke.voss@uni-konstanz.de

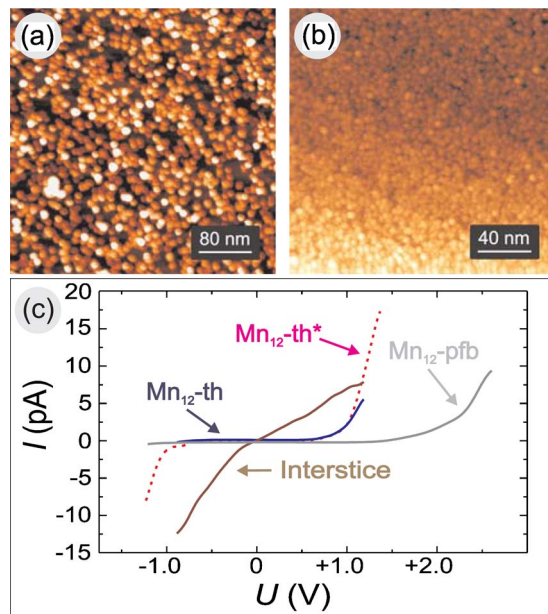


FIG. 1. (Color online) (a) $400 \times 400 \text{ nm}^2$ STM image of Mn_{12} -th clusters on the 4-MTBA functionalized Au(111) surface ($U=1 \text{ V}$; $I=6.9 \text{ pA}$). (b) $200 \times 200 \text{ nm}^2$ STM image of Mn_{12} -pfb on 4-MTBA/Au ($U=2 \text{ V}$; $I=6.9 \text{ pA}$). (c) Averaged I - U spectra taken at the center of Mn_{12} -th clusters at the center of Mn_{12} -pfb clusters and at interstices.

Figure 1(b) shows a STM image ($200 \times 200 \text{ nm}^2$) of Mn_{12} -pfb on 4-MTBA/Au. The homogeneity and the density of molecules are significantly increased compared with Mn_{12} -th. The characteristic monoatomic steps of Au(111) are still visible in the STM image despite the presence of a molecular layer. The Mn_{12} -pfb molecules appear smaller than the Mn_{12} -th clusters possibly due to a different apex radius of the STM tip used for this measurement.

Figure 1(c) shows I - U characteristics recorded at the center of Mn_{12} -th and Mn_{12} -pfb molecules as well as at positions between the Mn_{12} clusters (interstices). The I - U curves presented in this work were obtained by averaging over at least six spectra taken at different locations of the sample surface except for the dotted curve which represents a single measurement on Mn_{12} -th. The I - U characteristics taken at interstice positions show the features typical for aromatic thiols with an asymmetry between positive and negative bias voltages.^{23,24} Both I - U curves obtained at the center of Mn_{12} -th clusters show a line shape revealing a region of low conductivity (energy gap region) between -1.0 and $+0.8 \text{ V}$, as can be estimated from the signal slope edges of the spectrum marked with an asterisk. Increasing the bias voltages beyond -0.8 or 1.2 V during STS measurements on Mn_{12} -th leads to large instabilities in the I - U spectra. Typically with a fresh STM tip, only the first measurement could be performed in the range of $\pm 1.25 \text{ V}$ [dotted curve marked with an asterisk in Fig. 1(c)], whereas in all the consecutive measurements a maximum negative voltage of only -0.8 V could be applied for stable imaging. The possible reason for this could be a partial damage of the clusters upon imaging due to the current resulting in a decreased STM tip quality. For Mn_{12} -pfb the gap width is significantly increased with the onset of the empty states region shifted to about $+2 \text{ V}$. However, the maximum negative voltage for stable tunneling conditions was limited to about -1.3 V and thus the onset of the occupied states region could not be determined in case of Mn_{12} -pfb. The reason for the smaller gap width in case of

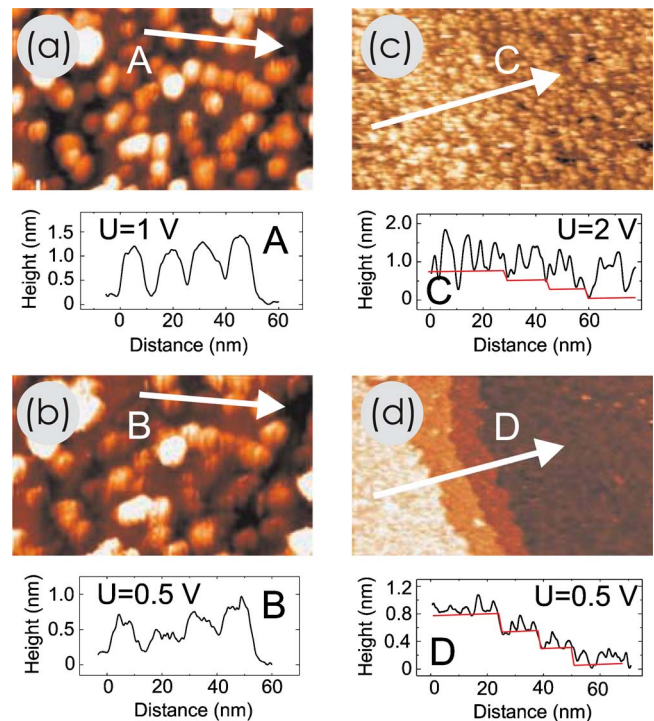


FIG. 2. (Color online) $120 \times 70 \text{ nm}^2$ STM images of Mn_{12} -th clusters taken at (a) $+1 \text{ V}$ and (b) $+0.5 \text{ V}$ bias voltages as well as of Mn_{12} -pfb clusters taken at (c) $+2 \text{ V}$ and (d) $+0.5 \text{ V}$ bias voltages. Corresponding height profiles are shown in the lower panels. In case of Mn_{12} -pfb the molecules are almost “invisible” for the STM operated at $+0.5 \text{ V}$ (within the band gap), and thus the characteristic steps of Au(111) (sketched in both height profiles) are visible.

Mn_{12} -th could be due to the different types of ligands.

In principle, the local density of states can be derived from STS measurements of the differential conductivity (dI/dU). However, in case of complex molecules bound to a substrate, the difference between the local value of the electrostatic potential and chemical potential is unknown. In relatively simple molecules this problem can be eliminated by using an extended Hückel model and a parameter η that describes how the electrostatic potential is divided between the two junctions.²⁵ Nevertheless, the determination of η requires a series of STS measurements with set voltages beyond the stability range of the investigated Mn_{12} clusters. Thus the analysis of the I - U curves of Mn_{12} clusters is limited to a qualitative interpretation. Despite these limitations, the I - U curves clearly show the presence of an energy gap in a spatially isolated individual Mn_{12} molecule, which structural integrity was verified before.¹⁹ These results also show a good agreement with the RPES measurements,^{18,19} which spatial resolution was, however, limited by the x-ray beam diameter of approximately $100 \mu\text{m}$.

Figure 2 shows STM images of Mn_{12} -th clusters [(a) and (b)] on 4-MTBA/Au(111) obtained at $+1$ and $+0.5 \text{ V}$ as well as of Mn_{12} -pfb clusters [(c) and (d)] on 4-MTBA/Au(111) obtained at $+2$ and $+0.5 \text{ V}$, respectively. The higher bias voltage corresponds to the onset of the unoccupied states region, whereas the lower value corresponds to the band gap region. When imaging within the broad gap region ($+0.5 \text{ V}$), the Mn_{12} -th molecules appear as round-shaped clusters with an apparent height of $0.5 \pm 0.2 \text{ nm}$, as shown in Fig. 2(b). In contrast, for the voltage at the band onset position (1 V), the Mn_{12} -th molecules appear much broader and

higher. The apparent height of the Mn₁₂-th clusters increases to 1.1 ± 0.2 nm for +1 V bias voltage that correlates with our previous results¹⁹ and is close to the expected height of 1.4 nm. In order to explain this fact, one needs to consider the tunneling from the occupied states of the STM tip into states of the Mn₁₂ molecule at higher bias voltage that results in a larger apparent height. At a lower bias voltage the electrons may tunnel directly from the tip to the conducting substrate and the molecular layer would only modulate the potential barrier as a function of position. A contrast due to the molecules might still be observed because the molecular overlayer can effectively lower the barrier. The height deviations between different clusters within one image can be attributed to different spatial orientations of the Mn₁₂-th clusters grafted to the 4-MTBA layer.

In case of Mn₁₂-pfb the molecules are almost “invisible” for the STM operated at +0.5 V bias voltage, and thus the characteristic monoatomic steps of Au(111) can be observed [Fig. 2(d)]. This can be assigned to the increased band gap width in case of Mn₁₂-pfb. At +2 V bias voltage the Mn₁₂-pfb molecules are visible [Fig. 2(c)] with an apparent height of 1.2 ± 0.1 nm, which is close to the expected height of 1.5 nm and consistent with the apparent height of Mn₁₂-th. The image quality in Fig. 2(c) is somewhat decreased compared with Fig. 1(b) due to the fact that the image [Fig. 2(c)] was obtained after a prolonged series of STS measurements and the STM tip was thus slightly contaminated.

From the consistency between topographic STM images and STS results, we conclude that the main features of the band gap of spatially isolated individual Mn₁₂ clusters were determined. Furthermore, there is a qualitative agreement between the STS measurements on Mn₁₂-th and break junction measurements of Ni *et al.*¹¹ on Mn₁₂ acetate, while there is a deviation in case of Mn₁₂-pfb that may be assigned to the different electronic properties of the respective ligands. The presence of a band gap in Mn₁₂ clusters is furthermore consistent with recent photoemission spectroscopy measurements on Mn₁₂-th,¹⁹ which revealed the onset of an energy gap about 1 eV below the Fermi level. The measured band gap width of Mn₁₂-th is close to the value obtained from LDA+*U* calculations for Mn₁₂.²⁰

In conclusion, we performed UHV STM/STS measurements at RT in order to determine the electronic structure of spatially isolated Mn₁₂-th and Mn₁₂-pfb molecules chemically grafted on the functionalized Au(111) surface. Reproducible current-voltage curves were obtained from both Mn₁₂ molecules showing a well defined wide band gap. A dependence of the energy gap width on the Mn₁₂ molecules' ligand shows up. In agreement with the tunneling spectroscopy results, the bias voltage variation upon scanning leads to apparent height changes of the Mn₁₂ clusters. Although the full electronic structure of Mn₁₂-th cannot be determined from our results we showed that chemically intact individual Mn₁₂ clusters exhibit an energy gap predicted by LDA+*U* calculations. In particular, a very good agreement between theory and experiment was found in case of Mn₁₂-th showing an experimental band gap value of about 1.8 eV. The results

contribute to the efforts of understanding the fundamental properties of Mn₁₂ SMMs on surfaces, which is necessary to integrate this material class in nanoscale storage devices or molecular electronics units.

The authors gratefully acknowledge support by the Deutsche Forschungsgemeinschaft (DFG) through Sonderforschungsbereich (SFB) 513. Two of the authors (M.B. and U.G.) are also grateful to the Merck KGaA and to the Wacker AG.

- ¹R. Sessoli, D. Gatteschi, A. Caneschi, and M. A. Novak, *Nature (London)* **365**, 141 (1993).
- ²T. Lis, *Acta Crystallogr., Sect. B: Struct. Crystallogr. Cryst. Chem.* **36**, 2042 (1980).
- ³A. Caneschi, D. Gatteschi, R. Sessoli, A. L. Barra, L. C. Brunel, and M. Guillot, *J. Am. Chem. Soc.* **113**, 5873 (1991).
- ⁴D. Gatteschi and R. Sessoli, *Angew. Chem., Int. Ed.* **42**, 268 (2003).
- ⁵M. N. Leuenberger and D. Loss, *Nature (London)* **410**, 789 (2001).
- ⁶L. Thomas, F. Lioni, R. Ballou, D. Gatteschi, R. Sessoli, and B. Barbara, *Nature (London)* **383**, 145 (1996).
- ⁷W. Wernsdorfer, M. Murugesu, and G. Christou, *Phys. Rev. Lett.* **96**, 057208 (2006).
- ⁸A. Naitabdi, J.-P. Bucher, P. Gerbier, P. Rabu, and M. Drillon, *Adv. Mater. (Weinheim, Ger.)* **17**, 1612 (2005).
- ⁹H. B. Heersche, Z. de Groot, J. A. Folk, H. S. J. van der Zant, C. Romeike, M. R. Wegewijs, L. Zoppi, D. Barreca, E. Tondello, and A. Cornia, *Phys. Rev. Lett.* **96**, 206801 (2006).
- ¹⁰M.-H. Jo, J. Grose, K. Baheti, M. M. Deshmukh, J. J. Sokol, E. M. Rumberger, D. N. Hendrickson, J. R. Long, H. Park, and D. C. Ralph, *Nano Lett.* **6**, 2014 (2006).
- ¹¹C. Ni, S. Shah, D. Hendrickson, and P. R. Bandaru, *Appl. Phys. Lett.* **89**, 212104 (2006).
- ¹²M. Mannini, D. Bonacchi, L. Zoppi, F. M. Piras, E. A. Speets, A. Caneschi, A. Cornia, A. Magnani, B. J. Ravoo, D. N. Reinhoudt, R. Sessoli, and D. Gatteschi, *Nano Lett.* **5**, 1435 (2005).
- ¹³A. Cornia, A. C. Fabretti, M. Pacchioni, L. Zoppi, D. Bonacchi, A. Caneschi, D. Gatteschi, R. Biagi, U. del Pennino, V. de Renzi, L. Gurevich, and H. S. J. van der Zant, *Angew. Chem.* **115**, 1683 (2003).
- ¹⁴L. Zoppi, M. Mannini, M. Pacchioni, G. Chastanet, D. Bonacchi, C. Zannardi, R. Biagi, U. del Pennino, D. Gatteschi, A. Cornia, and R. Sessoli, *Chem. Commun. (Cambridge)* **2005**, 1640.
- ¹⁵E. Coronado, A. Forment-Aliaga, F. M. Romero, V. Corradini, R. Biagi, V. de Renzi, A. Gambardella, and U. del Pennino, *Inorg. Chem.* **44**, 7693 (2005).
- ¹⁶B. Fleury, L. Catala, V. Huc, C. David, W. Z. Zhong, P. Jegou, L. Baraton, S. Palacin, P.-A. Albouy, and T. Mallah, *Chem. Commun. (Cambridge)* **2005**, 2020.
- ¹⁷G. G. Condorelli, A. Motta, M. Fevazza, P. Nativo, I. L. Fraga, and D. Gatteschi, *Chem.-Eur. J.* **12**, 3558 (2006).
- ¹⁸U. del Pennino, V. de Renzi, R. Biagi, V. Corradini, L. Zoppi, A. Cornia, D. Gatteschi, F. Bondino, E. Magnano, M. Zangrando, M. Zacchigna, A. Lichtenstein, and D. W. Boukhvalov, *Surf. Sci.* **600**, 4185 (2006).
- ¹⁹S. Voss, M. Fonin, U. Rüdiger, M. Burgert, U. Groth, and Y. S. Dedkov, *Phys. Rev. B* **75**, 045102 (2007).
- ²⁰D. W. Boukhvalov, M. Al-Sager, E. Z. Kurmaev, A. Moewes, V. R. Galakhov, L. D. Finkelstein, S. Chiuzaibaian, M. Neumann, V. V. Dobrovitski, M. I. Katsnelson, A. I. Lichtenstein, B. N. Harmon, K. Endo, J. M. North, and N. S. Dalal, *Phys. Rev. B* **75**, 014419 (2007).
- ²¹J. M. Lim, Y. Do, and J. Kim, *Eur. J. Inorg. Chem.* 711 (2006).
- ²²M. Burgert and U. Groth (unpublished).
- ²³A. I. Onipko, K.-F. Berggren, Y. O. Klymenko, L. Malysheva, J. J. W. M. Rosink, L. J. Geerligs, E. van der Drift, and S. Radellar, *Phys. Rev. B* **61**, 11118 (2000).
- ²⁴J. J. W. M. Rosink, M. A. Blauw, L. J. Geerligs, E. van der Drift, and S. Radelaar, *Phys. Rev. B* **62**, 10459 (2000).
- ²⁵S. Datta, W. Tian, S. Hong, R. Reifenberger, J. I. Henderson, and C. P. Kubiak, *Phys. Rev. Lett.* **79**, 2530 (1997).